Electron Photodetachment from Aqueous Anions. 2. Ionic Strength Effect on Geminate Recombination Dynamics and Quantum Yield for Hydrated Electron

Myran C. Sauer, Jr., Ilya A. Shkrob,* Rui Lian, Robert A. Crowell, and David M. Bartels†

Chemistry Division, Argonne National Laboratory, Argonne, Illinois 60439

Xiyi Chen, Diana Suffern, and Stephen E. Bradforth

Department of Chemistry, University of Southern California, Los Angeles, California 90089

Received: June 14, 2004; In Final Form: September 9, 2004

In concentrated solutions of $NaClO_4$ and Na_2SO_4, the quantum yield for free electron generated by detachment from photoexcited anions (such as I^-, OH^-, ClO_4^-, and SO_3^{2-}) linearly decreases by 6−12% per 1 M ionic strength. In 9 M sodium perchlorate solution, this quantum yield decreases by roughly 1 order of magnitude. Ultrafast kinetic studies of 200 nm photon induced electron detachment from Br^-, HO^-, and SO_3^{2-} and 228 nm photodetachment from I^- suggest that the yield of thermalized, solvated electron does not change in these solutions; rather, the ionic strength effect originates in more efficient recombination of geminate pairs. Within the framework of the recently proposed mean force potential (MFP) model of charge separation dynamics in such photosystems, the observed changes are interpreted as an increase in the short-range attractive potential between the geminate partners. Association of sodium cation(s) with the electron and the parent anion is suggested as the most likely cause for the observed modification of the MFP. Electron thermalization kinetics suggest that the cation associated with the parent anion (by ion pairing and/or ionic atmosphere interaction) is passed to the detached electron in the course of the photoreaction. The precise atomic-level mechanism for the ionic strength effect is presently unclear; any further advance is likely to require the development of an adequate quantum molecular dynamics model.

1. Introduction

In part 1 of this series,[1] estimates for absolute quantum yields (QYs) and cross sections for electron photodetachment from miscellaneous aqueous anions were given. With a single exception of perchlorate, these measurements were carried out in dilute (<50 mM) solutions of these CTTS (charge transfer to solvent) active anions. In this work, we explore the electron dynamics for photoexcited anions in high ionic strength solutions.

The motivation for such a study is provided by the recent ultrafast kinetic studies of electron photodetachment from halide [2−6] and pseudohalide[6−8] anions. These studies suggest the existence of a weak attractive mean force potential (MFP) between the residual radical (such as HO or a halogen atom) and the ejected electron that localizes in its vicinity. This attractive potential causes bimodality of the electron decay kinetics: in the first 10−50 ps, these kinetics are exponential (due to the fast escape and recombination of the electrons situated near the bottom of the potential well); [9] these rapid kinetics are succeeded by a slower $t^{-1/2}$ decay due to the diffusional escape and recombination of hydrated electrons which are thermally emitted from this potential well.[2,7,9] For polyvalent anions, only these slow kinetics are observed. In our studies of SO_3^{2-} and $Fe(CN)_6^{4-}$, the fast exponential component is lacking.[6,10] This is not surprising since long-range Coulomb repulsion between the electron and a radical anion (derived from the parent polyvalent anion) should be much stronger than short-range, weak attraction between the electron and a neutral radical (derived from the parent monovalent anion). For the latter type of geminate pairs, the MFP is thought to originate mainly through the polarization of the residue (e.g., halide atom) by the electron,[2,11,12] though the electron−dipole interaction may also be significant for pairs generated by electron photodetachment from polyatomic anions. Experiments from the USC group have shown that,[11] for geminate pairs derived from monovalent anions, the strength of the interaction (as estimated from MFP model kinetic fits) increases with the polarizability of the radical/atom, being at its maximum for iodine atoms. For chloride, the MFP has been obtained theoretically, using quantum molecular dynamics simulations and umbrella sampling by Staib and Borgis. [12] The strength of the simulated MFP between chlorine and the solvated electron (which is a few *kT* units) is comparable to the strength of the MFP that was extracted from the experimental kinetics for aqueous iodide. [2] Later work from Borgis and Staib, partly designed to mimic chlorine/electron pairs, simulated chloride/argon pairs in water and decomposed the *specific* interactions responsible for the MFP. [13] Although the MFP emerges as a sum total of many interparticle interactions, this study showed that the dominant part is due to the anion/polarizable atom pair interaction.

MFP models were found to quantitatively account for (i) the temporal profile of the geminate recombination kinetics,[2,6,7] (ii) the changes observed in these kinetics with increasing photoexcitation energy (direct ionization that occurs at higher energies broadens the spatial distribution of photoejected electrons),[14] and (iii) temperature effects on the decay kinetics of electrons

* To whom correspondence should be addressed. Tel: 630-252-9516. Fax: 630-2524993. E-mail: shkrob@anl.gov.

† Present address: Radiation Laboratory, University of Notre Dame, Notre Dame, IN 46556.

10.1021/jp047435j CCC: $27.50
Published on Web 10/26/2004

generated in 200 nm photoexcitation of hydroxide. [7] The MFP model also qualitatively accounts for the trends in the kinetics observed for homologous anions (e.g., the correlation between the potential well depth and the polarizability of the radical),[11] as well as some trends observed for nonaqueous[15] and mixed solvents.[3,4]

Impressive as this record may appear, there is no direct, unambiguous way in which the MFP profile can be extracted from the experimental data, and this leaves room for selecting the MFP parameters and the initial electron distribution to accommodate any of the trends observed. For example, to "explain" temperature effects on the geminate kinetics for (OH, e_{aq}^-) pairs generated in electron photodetachment from hydroxide, it was postulated that the MFP for this pair becomes shallower and more diffuse with increasing temperature.[7] Although the entire set of 8−90 °C kinetics can be consistently fit with these assumptions, there is currently no way of demonstrating experimentally that the MFP behaves as postulated. This uncertainty pertains to other studies: in the end, it is not yet clear whether the MFP model is a correct (though simplified) picture that captures peculiarities of electron dynamics for photoexcited CTTS anions or merely a recipe for producing kinetic profiles that resemble those observed experimentally.

We believe that the MFP model does capture the reality, albeit incompletely. The existence of a short-range interaction that temporarily stabilizes close pairs is also suggested by experimental[16−18] and theoretical[19] studies of Na^- CTTS by Schwartz and co-workers. These authors showed that electrons in the close pairs (observed on the short time scale)[16] responded differently to IR photoexcitation[17] than the electrons in more distant pairs. The short-term electron dynamics observed in the sodide photosystem has been viewed as the dissociation of these close pairs (in which the electron and sodium atom reside in a single solvent cavity) to solvent separated pairs (in which the species are separated by 1−2 solvent molecules) that subsequently decay by diffusional migration of the partners to the bulk.[16,17,19]

The purpose of the present study was to validate the use of the MFP model for aqueous anions. The approach was to modify this potential in a predictable way, through ionic atmosphere screening of electrostatic charges, an approach employed with some success for electron recombination after $Fe(CN)_6^{4-}$ detachment.[10] It was expected that, for geminate pairs derived from monovalent anions, the screening of the electron would weaken the electrostatic interactions of this electron with its neutral partner and the survival probability Ω_∞ of electrons that escape geminate recombination would thereby increase. Conversely, for polyvalent anions, this probability would decrease because the ionic atmosphere would screen the Coulomb repulsion between the electron and its negatively charged partner, the radical anion. As demonstrated below, these expectations were not realized.

The experimental results show that both the survival probability and the quantum yield of free electrons *decrease* with the ionic strength for all of the systems studied, whereas the prompt quantum yield for the electron does not change (by this "prompt" yield we mean the photoelectron yield attained at 2−3 ps after the excitation pulse, by the end of the solvation/thermalization stage). The magnitude of this decrease is the same for monovalent and divalent anions and changes little from one photosystem to another; it also varies little with the salt that is used to change the ionic strength. Although a similar magnitude of the decrease in the survival probability Ω_∞ of the electron with increasing ionic strength was attained for all photosystems, the rate for the attainment of this decrease varied considerably among different photosystems.

Though we cannot presently suggest a detailed model that accounts for these observations in their totality, it is certain that ion screening cannot account for these results even at the qualitative level. We suggest that the effect originates through the modification of the MFP via alkali cation association with the solvated electron and the parent anion; somehow, this association makes the short-range attraction stronger, for all anions.

In a closely related study, Lenchenkov et al. studied the effect of addition of 0.04−4 M KBr on the dynamics of ($Fe(CN)_6^{3-}$, e_{aq}^-) pairs generated by 255 nm photoexcitation of hexacyanoferrate(II) anion (ferrocyanide).[10,20] For ferrocyanide CTTS, a 4% decrease per 1 M of KBr in the survival probability of geminate ($Fe(CN)_6^{3-}$, e_{aq}^-) pairs (extrapolated from the kinetic data obtained for $t < 400$ ps) was observed. As ion association is particularly strong and documented in solutions of ferrocyanide, association of ferrocyanide with 1−3 potassium cations was suggested to reduce the Coulomb repulsion between the geminate partners.[10] The results can also be interpreted in terms of ionic atmosphere screening or a self-consistent combination of screening and ion association.[20] As seen from the results of the present work, the ionic strength effect occurs even for geminate pairs in which no Coulomb repulsion exists. Nevertheless, we believe that the root cause of this effect is the same for all photoexcited anions: the short-range MFP (which may or may not include Coulomb repulsion) is modified by the ion association.

In the view of this latter conclusion, most of this paper constitutes an extended proof of the assertions given above. That task required combining several spectroscopic techniques, including pulse radiolysis, laser flash photolysis, and ultrafast pump−probe spectroscopy. To reduce the length of the paper, additional experimental data and analyses that substantiate our results have been placed in the Supporting Information.

2. Experimental Section

Nanosecond Flash Photolysis and QY Measurement. The setup used to determine the QY for free electron formation has been described in part 1 of this series.[1] Fifteen nanosecond fwhm, 1−20 mJ pulses from an ArF (193 nm) or KrF (248 nm) excimer laser (Lambda Physik LPX 120i) were used to photolyze N_2-saturated aqueous solutions. The laser and analyzing light beams were crossed at an angle of 30° inside a 1.36 mm optical path cell. A fast silicon photodiode equipped with a video amplifier terminated into a digital signal analyzer were used to sample the transient absorbance kinetics (>3 ns). Two pyroelectric energy meters were used to measure the power of the incident and transmitted UV light during the kinetic sampling. A total of 200−500 mL of the solution being studied was circulated through the cell using a peristaltic pump. The typical flow rate was 2−3 mL/min; the repetition rate of the laser was 1.25 Hz. Purified water with a conductivity of <2 nS/cm was used to prepare the aqueous solutions. The UV spectra were obtained using a dual beam spectrophotometer (OLIS/Cary 14).

The typical QY measurement included determination of laser transmission T through the sample, transient absorbance ΔOD_λ of the photoproduct at wavelength λ of the analyzing light, the laser energy I_{abs} absorbed by the sample, and the incident beam energy I_0. The QY was determined from the initial slope of ΔOD_λ vs I_{abs} that was corrected for the window transparency and noncollinear beam geometry. If not stated otherwise, the

absorbance of hydrated electron at $\lambda = 700$ nm ($\epsilon_{700} = 20560$ M^{-1} s^{-1})[21,22] at the end of the UV pulse ($t = 30$ ns) was used to estimate the electron yield. The anion concentration and light fluence were chosen so that the decay half time of this electron (due to cross recombination) was >5 μs. Supporting experiments designed to establish the effect of salts on the hydrated electron spectrum were carried out by pulse radiolysis;[16] details are given in section 1S.

Ultrafast Laser Spectroscopy. The femtosecond kinetic measurements at Argonne were obtained using a 1 kHz Ti:sapphire laser setup whose details are given in refs 7 and 8. Stretched 2 nJ pulses from a Ti:sapphire oscillator were amplified to 4 mJ in a home-built two-stage multipass Ti:sapphire amplifier. The amplified pulses were passed through a grating pair compressor that yielded Gaussian pulses of 60 fs fwhm and 3 mJ centered at 800 nm. The amplified beam was split into three parts of approximately equal energy. One beam was used to generate 800 nm probe pulses while the other two were used to generate the 200 nm (fourth harmonic) pump pulses by upconversion of the third harmonic. Up to 20 μJ of the 200 nm light was produced this way (300−350 fs fwhm pulse). The pump and probe beams were perpendicularly polarized, focused to round spots of 50 μm and 200−300 μm in radius, respectively, and overlapped in the sample at 6.5°. Commonly in the pump−probe experiments, the pump beam envelopes the probe beam. We reversed this geometry because of the poor quality of the 200 nm beam ("hot spots" in the beam profile). This reverse geometry minimizes the sensitivity of the absorption signal to fluctuations of the "hot spot" pattern and the walk-off of the probe beam relative to the pump beam (which was typically 5−10 μm). The tradeoff was a considerable reduction in the signal magnitude that was more than compensated by improved signal-to-noise ratio and shot-to-shot stability.

The probe and the reference signals were detected with fast silicon photodiodes, amplified, and sampled using home-built electronics. The typical standard deviation for a pump−probe measurement was 10^{-5} ΔOD, and the "noise" was dominated by the variation of the pump intensity and flow instabilities in the jet. The vertical bars shown in the kinetics represent 95% confidence limits for each data point. Typically, 150−200 points acquired on a quasi-logarithmic grid were used to obtain these kinetics. The experiments were carried out in flow, using a 150 μm thick high-speed jet. An all 316 stainless steel and Teflon flow system was used to pump the solution.

The experiments at the University of Southern California were carried out using a 200 kHz Ti:sapphire amplified laser system and a pump−probe spectrometer which have been described elsewhere.[3−5,10] Briefly, the regenerative amplifier produces pulses of 60 fs fwhm at 800 nm. A small fraction of the fundamental is split off for use as a probe while the remainder is frequency doubled to 400 nm to drive an optical parametric amplifier (OPA). A total of 228 nm pulses (5 nJ) are generated by sum frequency mixing the signal output of the OPA with the residual 400 nm light. The perpendicularly polarized pump and probe beams at the sample were focused to 50 and 35 μm diameter spots, respectively. The solutions were flowed through a 200 μm optical path Suprasil cell. The instrument response function for both spectrometers is 350 fs or better.

Materials and Solution Properties. Reagents of the highest purity available from Aldrich were used without further purification. The solutions were made of crystalline salts with the exception of hydroxide solutions, which were made using high-purity 0.989 N analytical standard KOH.

Density, viscosity, activity, and ion diffusivity charts for sodium sulfate and sodium perchlorate solutions were taken from the literature (some of the relevant data are given in Figures 1S−3S in the Supporting Information).[24,25] In saturated room-temperature solution, these molarities and the densities are 1.84 M and 1.21 g/mL for sodium sulfate and 9.32 M and 1.68 g/mL for sodium perchlorate, respectively.[25] The refractive indices of these solutions change very little relative to that of neat water (at saturation, 1.368 for $NaClO_4$[26] and 1.364 for Na_2SO_4[27] vs 1.333 for water;[27] for the sodium line). The density of the solution scales approximately linearly with the molarity of the salt (Figures 1S(a) and 3S(a)).[24] This increase in the density results in a higher stopping power for 20 MeV electrons in concentrated solutions and has important implications for pulse radiolytic experiments (section 1S). The quantity that changes most with the salinity is the bulk viscosity: from 1 cP for water to 1.9 cP for sodium sulfate (Figure 1S(a)) and to 8 cP for sodium perchlorate (Figure 3S(a)), for saturated solutions (for the latter salt, most of the increase in the viscosity occurs between 6 and 9 M, Figure 3S(a)). Microscopic diffusion coefficients for the corresponding ions change less than these bulk viscosities.[24] In 2.5 M $NaClO_4$ and 1.8 M Na_2SO_4, the sodium cation migrates ca. 30% more slowly than in water (Figures 1S(b) and 3S(b)). In 0.5−2 M Na_2SO_4, the diffusion coefficient of sulfate is constant, also ca. 30 % lower than in water (Figure 1S(b)). Thus, the drag of the ionic atmosphere on the migration of these ions is relatively weak. The (nominal) ionic strength given below in section 3 was calculated assuming the absence of ion pairing. For sodium sulfate, Raman spectroscopy,[28] dielectric permittivity,[29] ultrasonic absorption,[30] and conductivity[31] studies suggest the occurrence of noncontact ion pairs in which the sulfate anion and the sodium cation are separated by one or two water molecules. Since the ion activities rapidly decrease with the salt concentration (Figure 2S(a)),[29] the association constant decreases by 2 orders of magnitude from dilute to saturated solution (see Figure 3 in ref 23), and ion pair formation peaks at ca. 0.2 M (Figure 2S(b)).[29] When this ion pairing is included, the ionic strength of the Na_2SO_4 solutions is ca. 2.83 times the molarity of the sodium sulfate (Figure 2S(b)).

3. Results

This section is organized as follows. First, the choice of (inert) salts used to change the ionic strength of CTTS anion solutions under study is justified. It is shown that only two types of such salts, perchlorates and sulfates, can be used for studies of the ionic strength effect in the CTTS photosystems (section 3.1). The addition of these salts shifts the absorption spectra of CTTS anions and the hydrated electron to the blue (sections 3.2 and 1S, respectively). Since the molar absorptivities of the parent anion and the electron are therefore concentration dependent, this spectral shift has to be taken into the account for our QY measurements. The effect of salts on the spectrum and molar absorptivity of the electron are examined in sections 1S and 2S in the Supporting Information. The latter data suggest that the oscillator strength of the s → p transition in the visible does not change with the ionic strength. Using the estimates for ϵ_{700} obtained therein, absolute quantum yields, ϕ, were obtained as a function of the ionic strength I (section 3.3). All of these dependencies were linear, with a negative slope of 6−12% per 1 M of ionic strength. Ultrafast pump−probe spectroscopy was used to demonstrate that this effect originates through a perturbation in the recombination dynamics of the corresponding geminate pairs; there is no ionic strength effect on the *prompt*

yield of photoelectrons in the CTTS excitation (section 3.4). The kinetics for electron photodetachment from bromide and iodide are analyzed using an MFP model of geminate recombination based on the work of Shushin. [7,9] These analyses suggest that the short-range attractive potential between the geminate partners increases with ionic strength.

3.1. Choice of the Ion Atmosphere. In our experiments, the ionic strength of aqueous solutions was changed by addition of sodium sulfate and sodium perchlorate. This choice was dictated by the following practical considerations.

First, most anions are reactive toward the radical generated in the course of electron photodetachment. Typical reactions include addition (e.g., halogen atoms and OH radicals readily add to halide anions) and oxidation (OH, SO_3^-, and SO_4^- are very strong oxidizers). Sulfate and perchlorate are two isoelectronic anions for which no addition or oxidation reactions have ever been reported. This guarantees that the salts used for changing the ionic strength are not *chemically* involved in the electron detachment and/or geminate recombination.

Second, the anions must be sufficiently weak absorbers of photoexcitation light, even at molar concentration of these anions, so that most of the photoexcitation light is absorbed by the CTTS anions of interest which are present in a relatively low concentration. The latter consideration forced us to use CTTS anions that were good light absorbers ($\epsilon > 500$ M^{-1} cm^{-1}) at the photoexcitation wavelength, such as iodide at 248 and 228 nm and hydroxide at 193 nm (see Table 1 in ref 1) and to use sufficiently high concentrations of these anions so that <0.1% of the light was absorbed by the buffer salt (in flash photolysis experiments). Nanosecond observations suggested that neither sulfate nor perchlorate yield electrons by single 248 nm photon excitation, even in saturated solutions (the QY is $<10^{-4}$). For 193 nm photoexcitation, because sulfate is a relatively strong light absorber ($\epsilon_{193} = 46 \pm 7$ M^{-1} cm^{-1}),[1] only perchlorate can be used ($\epsilon_{193} = 0.565 \pm 0.007$ M^{-1} cm^{-1}).[1]

3.2. Effect of Salts on the CTTS Bands of Anions. It is known from previous studies that addition of salts to water shifts the CTTS absorption bands of anions to the blue. According to Blandamer and Fox[32] and Stein and Treinin,[33] this shift changes neither the shape of the absorption band nor the molar absorptivity of the anion at the band maximum. The latter authors studied the effect of $NaClO_4$ and Na_2SO_4 on the absorption of aqueous iodide; however, only band maxima positions were reported. To obtain more detailed data, UV spectra of 0.7 mM NaI in 1 mm and 10 mm optical path cells were collected as a function of salt concentration. For $\lambda > 205-210$ nm, the (low energy sub-) band was perfectly Gaussian; the bandwidth (314 ± 4 meV) and the molar absorptivity at the maximum (1.1×10^4 M^{-1} cm^{-1}) changed <2% with the salt concentration (Figure 1a). For both salts, the blue shift ($-\Delta\lambda$) linearly increased with the nominal ionic strength, and the band shifts given by Stein and Treinin[33] were in perfect agreement with those obtained in this work (Figure 1b). In energy units, the band shifts for sodium perchlorate and sodium sulfate are 26 and 13.4 meV per 1 M ionic strength. Thus, in 9 M $NaClO_4$ solution, the band shift is ca. 10 nm. Such a large shift strongly changes the molar absorptivity of the anion at the low energy band tail. Figure 1c shows the plot of the molar extinction coefficient ϵ_{248} of iodide at 248 nm as a function of the ionic strength. These data were obtained from spectrophotometric data of Figure 1a and compared with values estimated from the transmission of 248 nm light from the KrF laser. These two methods gave similar results: As seen from this plot, an increase in the ionic strength causes a large decrease in the molar absorptivity. For 9 M $NaClO_4$ solution, the molar absorptivity of iodide decreases by more than a decade. Only for this $I^-/NaClO_4$ photosystem was the blue shift sufficiently large to produce nonlinear dependence of the molar absorptivity (at the band edge) on the salt concentration. For other photosystems studied at 248 and 193 nm, the molar absorptivity linearly decreased with the salinity. For hydroxide at 193 nm (where the anion has a band maximum), the molar absorptivity changed from 3000 M^{-1} cm^{-1} in water to 900 M^{-1} cm^{-1} in 9 M $NaClO_4$ solution (see Figure 4S). For sulfite at 248 nm, the molar absorptivity changed from 40 M^{-1} cm^{-1} in water to 25 M^{-1} cm^{-1} in 1.8 M Na_2SO_4 (see Figure 4S). Thus, for all photosystems (including 200 nm photosystems), the absorptivity of the solution at the excitation wavelength systematically decreases with the ionic strength.

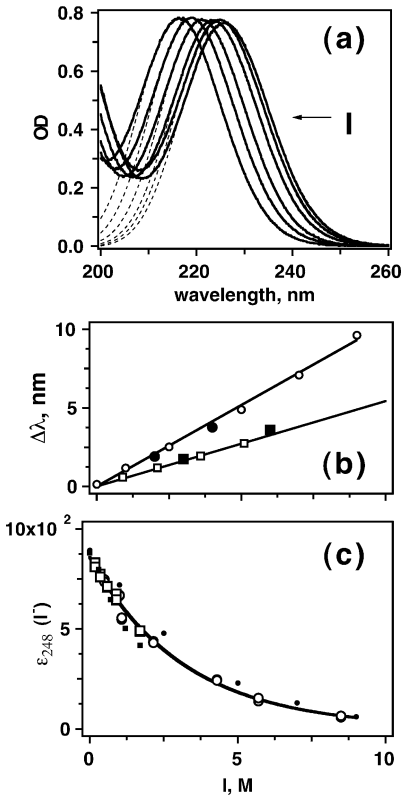

Figure 1. (a) Solid lines: Absorption spectra of 0.7 mM NaI vs sodium perchlorate concentration (1 cm optical path cell). The molar concentrations of the perchlorate (from right to left) are 0, 1, 2.5, 5, 7, and 9 M (the direction of the increase in the ionic strength *I* is indicated with an arrow in the plot). Dashed lines are the Gaussian fits to these absorption spectra. (b) Negative shift $\Delta\lambda$ of the band maximum for aqueous iodide vs the nominal ionic strength of sodium perchlorate (circles) and sodium sulfate (squares). Empty symbols indicate the data obtained in the present work; filled symbols are data taken from ref 33. (c) Molar absorptivity of aqueous iodide at 248 nm (given in the units of M^{-1} cm^{-1}) vs the salinity of photolyzate (that was changed by addition of $NaClO_4$ and Na_2SO_4). The circles are for sodium perchlorate and the squares are for sodium sulfate solutions. The filled symbols are spectrophotometric data from (a); the empty symbols are 248 nm laser transmission data (sections 2 and 3.4). The solid line is an exponential fit.

As shown in section 1S in the Supporting Information (see also Figures 5S and 6S and refs 34−36), addition of salts blue-shifts the s → p absorption band of hydrated electron in a manner similar to that of the anion CTTS bands. This effect has to be taken into account when the quantum yield of electron photodetachment is estimated.

3.3. Quantum Yields for Electron Photodetachment by 248 and 193 nm Light. As explained in section 1S, the absolute

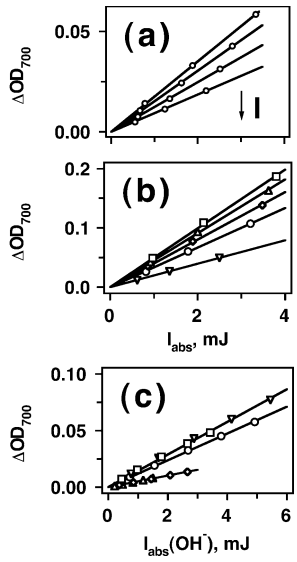

Figure 2. Transient absorption of photoelectrons (observed at 700 nm) vs absorbed laser power. The direction of increase in the nominal ionic strength I of photolyzed solution is indicated by an arrow. The solid lines drawn through the data points are linear fits. (a) Electron absorbance in 248 nm laser photolysis of 38.5 mM sulfite in (from top to bottom) 0.36, 0.73, 1.19, and 1.73 M sodium sulfate and (b) 2 mM iodide in (from top to bottom) 0.174 M (squares), 0.353 M (triangles), 0.59 M (diamonds), 0.9 M (circles), and 1.7 M (upturned triangles) sodium sulfate. (c) Electron absorbance in 193 nm laser photolysis of hydroxide in (from top to bottom) 2.1, 4.5, and 9 M sodium perchlorate vs the laser power $I_{abs}(OH^-)$ absorbed by the hydroxide. [KOH] was 0.75 mM (squares) and 1.5 mM (triangles) for 2.1 M $NaClO_4$ series, 0.75 mM (squares) and 1.5 mM (upturned triangles) for 2.1 M $NaClO_4$ series, 2 mM (circles) for 4.5 M $NaClO_4$ series, and 1 mM (triangles) and 2 mM (diamonds) for 9 M $NaClO_4$ series.

extinction coefficient ϵ_{700} of the hydrated electron in saline solutions is not known accurately since the absorption spectrum changes with salinity. Therefore, we first determine the quantity Φ_{rel} (the ratio of photodetachment cross sections) given by

$$\Phi_{rel} = \frac{\phi}{\phi(I=0)} \frac{\epsilon_{700}}{\epsilon_{700}(I=0)} \qquad (1)$$

where I is the ionic strength. This quantity can be determined directly from the plots of end-of-pulse transient absorbance of the electron at 700 nm (ΔOD_{700}) vs the absorbed laser power I_{abs}. Typical plots for 38.5 mM sulfite and 2 mM iodide in Na_2SO_4 solution are shown in Figure 2, parts a and b, respectively. All of the photosystems exhibited linear dependencies of ΔOD_{700} vs I_{abs} so that the product $\phi\epsilon_{700}$ can be readily obtained from the slopes of the corresponding plots. These $\phi\epsilon_{700}$ products were then plotted vs the ionic strength of the solution; all such dependencies were linear. Extrapolation of these linear dependencies to zero ionic strength gave the estimate for the product $\phi(I=0)\,\epsilon_{700}(I=0)$ by which Φ_{rel} (eq 1) was calculated. The estimates for $\phi(I=0)$ that were obtained in this work using the known molar absorptivity of hydrated electron in dilute aqueous solutions were within 3% of the values reported in Table 1, ref 1.

One of the photosystems studied, $OH^-/NaClO_4$ excited by 193 nm light, needed special treatment, because some of the excitation light was absorbed by sodium perchlorate (Figures 2c and 7S). As shown in part 1 of this series,[1] perchlorate yields electrons by one- or two- 193 nm photon excitation (the one-photon QY is 4×10^{-3}). Since the absorption band of perchlorate shifts to the blue with the perchlorate concentration, at least 20−50% of the 193 nm light is absorbed by 1−2 mM hydroxide, even in 9 M $NaClO_4$ solution. In dilute aqueous solution, the QY for hydroxide is ca. 0.11,[1,37,38] and <3% of the electron absorbance signal was from perchlorate, for all concentrations of the latter. Still, corrections were necessary to determine QYs for the $OH^-/NaClO_4$ photosystem, as the extra 193 nm absorbance by perchlorate has the effect of reducing the apparent electron yield. To compensate for this effect, the absorbance OD_{193} of the solution at 193 nm was determined and plotted as a function of hydroxide concentration (Figure 7S). These dependencies were linear and exhibited a positive offset at $[OH^-] = 0$ (due to the light absorbance by perchlorate), from which the fraction of photons absorbed by hydroxide can be estimated (as the ratio of hydroxide absorbance $OD_{193}(OH^-)$ to the total absorbance). The absorbed laser power I_{abs} was corrected by this ratio giving the laser power $I_{abs}(OH^-)$ absorbed by hydroxide alone: $I_{abs}(OH^-) = I_{abs}(OD_{193}(OH^-)/OD_{193})$. As shown in Figure 2c, when ΔOD_{700} is plotted against this latter quantity, the points obtained for different hydroxide concentrations are on the same line, which justifies the whole approach.

Figure 3a gives the resulting plots of Φ_{rel} as a function of the ionic strength (the data for electron photodetachment from perchlorate itself[1] are also included). It is seen that the decrease in Φ_{rel} is similar for all four of the CTTS anions being studied (varying from 6 to 10% per 1 M ionic strength) in either sodium sulfate and sodium perchlorate solutions. Examination of Figure 3a suggests that Φ_{rel} decreases mainly due to a decrease in the *absolute* QY for electron photodetachment; the change in the molar absorptivity of the hydrated electron is relatively unimportant. Indeed, in 9 M $NaClO_4$, Φ_{rel} for iodide is ca. 20 times lower than in water, whereas the estimated decrease in ϵ_{700} is just 20% (Figure 3b and section 1S). For 1.7 M Na_2SO_4, Φ_{rel} is ca. 0.4 whereas the estimated decrease in ϵ_{700} is just 5%. As demonstrated in section 2S, the changes in the electron absorptivity at 700 nm with increasing salinity are as small as suggested by our pulse radiolysis data in section 1S, and the decrease in the absolute QY for electron photodetachment is as large as suggested by the data of Figures 3a and 6S. To prove that, the yield-absorptivity products for hydrated electron and I_2^- anion generated in electron photodetachment from aqueous iodide were determined as a function of ionic strength (section 2S and Figure 8S therein). Assuming that the absorptivity of I_2^- [39,40] does not change with salinity (as suggested by the data in section 2S), the ratio $\epsilon_{700}/\epsilon_{700}(I=0)$ for hydrated electron was obtained (section 2S and Figure 3b). Using this ratio, the ratios $\phi/\phi(I=0)$ were estimated from the data shown in Figure 3a using eq 1 (Figure 3c). Since the decrease in the electron absorptivity with ionic strength is relatively small, the two plots (Figure 3, parts a and c) look very similar.

To summarize these QY data, the quantum yield of electron photodetachment rapidly decreases with increasing ionic strength of the solution (Figure 3c). The magnitude of the decrease in the QY per 1 M ionic strength is similar for all of the photosystems studied. Note that the decrease in the molar absorptivity of CTTS anions with the ionic strength has already been factored into the calculation of the QYs since we directly measured the absorption of the excitation light by these solutions. The concomitant decrease in the molar absorptivity of the electrons at 700 nm has also been taken into account, as explained above.

It should be stressed that we are not first to look for the ionic strength effect on the electron yield.[41,42] These previous studies were excluded from our consideration so far because we believe that the data were compromised by inadequate choice of anion

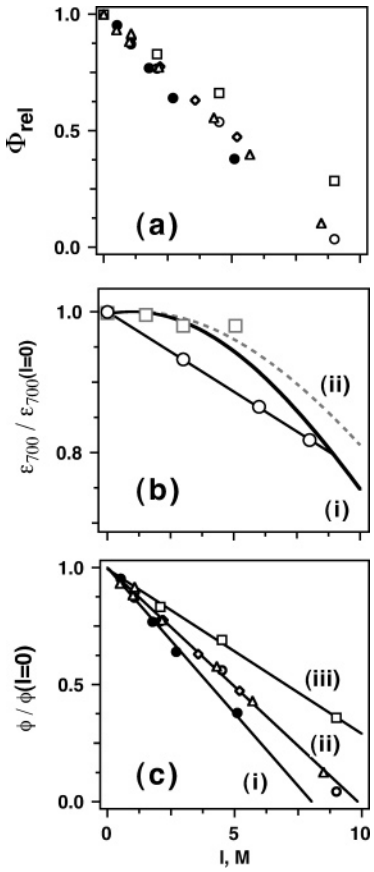

Figure 3. (a) Relative cross section Φ_{rel} of electron photodetachment (given by eq 1) as a function of the nominal ionic strength I of iodide (filled circles) and sulfite (empty diamonds) in sodium sulfate solutions and iodide (empty triangles) in sodium perchlorate solutions and 193 nm photoexcitation of perchlorate (empty circles) and hydroxide (empty squares) in sodium perchlorate solutions. (b) Ionic strength dependence of relative molar absorptivity $\epsilon_{700}/\epsilon_{700}(I = 0)$ of solvated electron at 700 nm in sodium perchlorate (circles) and sodium sulfate (squares) solutions obtained as explained in section 2S. The solid (i) and dashed (ii) lines (for perchlorate and sulfate, respectively) were calculated from the data of Figure 6S(b) assuming the constancy of the oscillator strength of the corresponding optical transition. (c) Relative quantum yield $\phi/\phi(I = 0)$ of electron photodetachment vs I for the anions shown in plot (a) (same notation). The linear plots (solid lines marked (i), (ii), and (iii)) correspond to decreases of 11%, 9.8%, and 6.2% per 1 M ionic strength, respectively.

photosystems. In particular, Jortner et al.[41] claimed the absence of the effect for 254 nm photoexcitation of aqueous iodide. Specifically, they looked for an effect of addition of 2.5 and 5 M HCl on the evolution of H_2 from a solution that contained 0.15 M iodide and 9 M LiCl. In a different experiment, the effect of the addition of 1 M KBr on the formation of iodine in N_2O-saturated solution containing 0.15 M KI and 1.8 M H_2SO_4 was sought. It is difficult to interpret these data since in both of these cases the reference systems were also concentrated solutions. Furthermore, under the experimental conditions, Cl^- and Br^- reacted with iodine atoms and hydrated electrons reacted with hydronium ions on a subnanosecond time scale; that is, the geminate dynamics were perturbed in a major way. Ohno[42] observed that in 254 nm photoexcitation of ferrocyanide the electron yield estimated from N_2 evolution in N_2O saturated solution decreased linearly with the concentration of sodium sulfate and sodium perchlorate (<1 M) added to the reaction mixture (19% and 32% decrease per 1 M of ionic strength, respectively). This decrease is much greater than shown in Figure 3c; however, $Fe(CN)_6^{4-}$ is known to strongly associate with 1−3 alkali cations,[10,20] even in dilute solutions,[10,43] and in that propensity, it is different from the anions studied herein. Furthermore, the absolute QYs obtained for $Fe(CN)_6^{4-}$ by Ohno[42] are 2 times lower than any other published estimate for this quantum yield (see Tables 1 and 4 in ref 1).

The QYs determined using flash photolysis are quantum efficiencies for the formation of a *free* electron that escaped recombination with its geminate partner. This quantity is given by the product of a prompt QY for the electron formation (which depends on the details of dissociation of a short-lived CTTS state on subpicosecond time scale) and a fraction Ω_∞ of electrons that escape geminate recombination on a subnanosecond time scale. It is not obvious from the data of Figure 3c, which one of these two factors is responsible for the observed decrease in the (free) electron yield with the increased ionic strength. The previous observations of an ionic strength effect on the quantum efficiency of electron detachment from $Fe(CN)_6$,$^{4-}$ by Ohno,[42] were interpreted by the author as the effect of solvent cage constriction around the CTTS state; in other words, the decrease in the yield of free electrons was thought to result from the decrease in the *prompt* electron yield attained in the course of this CTTS state dissociation. This interpretation is at odds with the recent results of Lenchenkov et al.[10,20] for the same ferrocyanide photosystem suggesting that addition of KBr changes the escape fraction Ω_∞ of the photoelectrons rather than their prompt quantum yield.

In the next section, ultrafast spectroscopy is used to demonstrate that the ionic strength effect is dynamic in origin and develops on the time scale of hundreds of picoseconds; the prompt electron yield does not change with the salt concentration.

3.4. Ultrafast Pump−Probe Spectroscopy of Anions in Concentrated Solutions. *3.4.1. Bromide and Iodide.* We have seen in the previous section that the electron quantum yield from I^- is strongly dependent on ionic strength. Let us now consider how ionic strength alters the time-dependent geminate recombination observed after halide anion photodetachment. Bradforth's group has in earlier work studied the effect of KI concentration on the geminate recombination dynamics of ($I^\bullet$, e_{aq}^-) pair and found no concentration effect up to 0.2 M.[4] Here we examine the much higher ionic strength range where an effect is observed in the overall quantum yield.

Bromide has an absorption maximum at 200 nm,[32] and blue shift of the absorption band with the ionic strength has relatively little effect on the molar absorptivity of this anion at the photoexcitation wavelength.[44] Due to the large absorptivity of this anion at 200 nm (10^4 M^{-1} cm^{-1}), photoexcitation of sulfate and perchlorate is negligible in the 20−80 mM NaBr solutions that were used (see section 3S in the Supporting Information). Likewise, when iodide is photoexcited at 228 nm, which is near the CTTS band peak (see Figure 1a), the absorption by perchlorate is negligible. We note that 228 nm rather than 200 nm excitation was chosen for I^- as 200 nm photoexcitation (which lies in the second CTTS band) leads to some direct ionization which competes with the CTTS photoprocess and modifies the geminate recombination kinetics. [14] For bromide, there is no variation in detachment dynamics at 200 and 228 nm, i.e., across the low-energy CTTS subband (see part 3 of this series).[6]

Typical 800 nm transient absorption kinetics obtained from 30 mM bromide and 10 mM iodide in sodium perchlorate solutions are given in Figure 4(a) and Figure 5(a), respectively. Additional data for bromide in sulfate solutions are shown in Figures 11S and 12S. The initial very rapid kinetics (t < 3 ps)

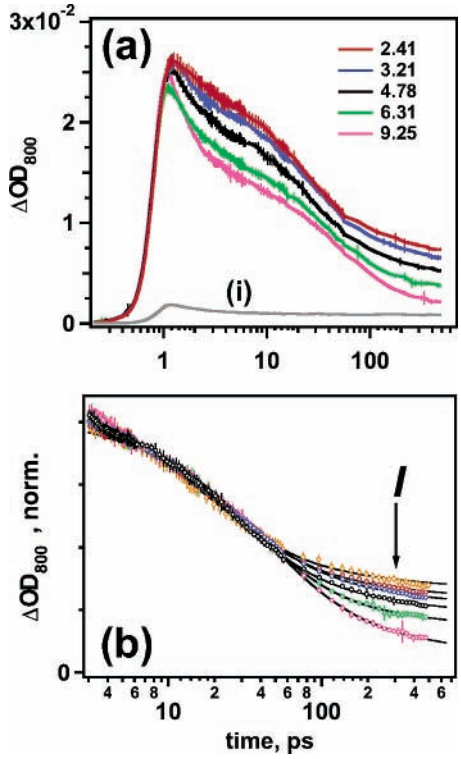

Figure 4. (a) 200 nm pump−800 nm probe transient absorption kinetics of electron in photolysis of 30 mM NaBr in solution containing 2.4 to 9.25 M sodium perchlorate. The molarity of $NaClO_4$ is indicated in the color scale. Absorption signal (i) is from 9.3 M perchlorate with no bromide added (under the same excitation conditions). The absorption of 200 nm photoexcitation light by perchlorate in the bromide solutions was negligible. The vertical bars are 95% confidence limits. (b) The same kinetic data (circles) normalized at $t = 5$ ps (the upper trace is for aqueous bromide with no $NaClO_4$ added). The same color coding used as in (a); the direction of the increase in the nominal ionic strength I is indicated by an arrow. The solid lines drawn through the symbols are simulations using Shushin's theory (section 3.4.3) with the parameters given in Figure 6.

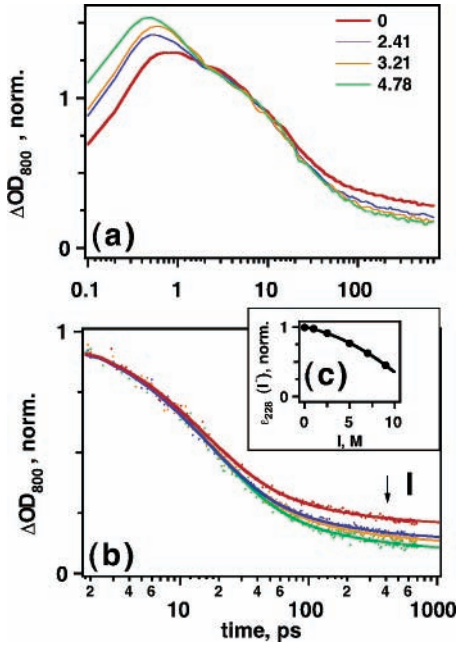

Figure 5. (a) Normalized 228 nm pump−800 nm probe kinetics of photoelectron generated by photolysis of 10 mM NaI in concentrated sodium perchlorate solutions. The molarity of perchlorate is given in the legend. These kinetics were polynominally smoothed and normalized at $t = 5$ ps. (b) Normalized decay kinetics of hydrated electron generated by 228 nm photoexcitation of 10 mM NaI in (from top to bottom) 0, 2.41, 3.21, and 4.78 M $NaClO_4$ (scattered dots; no smoothing). See also Figure 6a, trace (ii). The solid lines are the least-squares fits obtained using Shushin's theory equations. (c) As shown in the inset, the molar absorptivity of iodide at 228 nm rapidly decreases with increasing [$NaClO_4$]. For this reason, the prompt ΔOD_{800} signal from the electron obtained by 228 nm photoexcited 10 mM iodide solution also decreases with increasing [$NaClO_4$].

are from electron thermalization and solvation. For higher concentrations of $NaClO_4$, these kinetics become progressively faster and the optical density at 5−10 ps systematically decreases. Both of these trends are due to shifting of the absorption band of the thermalized electron to the blue (section 1S). The decrease in the prompt signal from the presolvated electron with $NaClO_4$ concentration is relatively small (because the absorptivity of this presolvated species changes little with the ionic strength). In water, the maximum of the electron band is ca. 719 nm, [22,36] which is close to our probe wavelength (800 nm). In 9 M $NaClO_4$, this band maximum shifts to 636 nm (section 1). From previous studies of electron thermalization in water photoionization[45−47] and iodide photoexcitation,[3] it is known that the band maximum of the presolvated electron systematically shifts to the blue in the first 500−800 fs. After the first 2 ps, this maximum reaches its equilibrium position[3,45,47] In the photoionization of neat water, [45] further spectral evolution is due to narrowing of the band to the red of the band maximum and widening of the band to the blue of the band maximum.[45,46] The greater the observation wavelength with respect to this maximum is, the greater the reduction in the electron absorbance during the thermalization process is and the faster the thermalization kinetics is.[45] This can be demonstrated by changing the observation wavelength[45,46] or by increasing the temperature of the solution (the spectrum of hydrated electron shifts to the red with increasing temperature, and the effect is exactly opposite to that shown in Figures 4a and 5a). [47,48] The decrease of the 800 nm absorbance at the end of the thermalization process (at 5−10 ps) with [$NaClO_4$] reflects the decrease in the molar absorptivity of hydrated electron; when the latter is taken into account using the data obtained in section 1S (see Figure 13S(a)), there is little variation in the yield of the thermalized electron at 5−10 ps (Figure 13S(b)).

In Figures 4b and 5b, the same kinetics resulting from electron detachment from the two anions have been normalized at 5 ps (by which time the spectral evolution due to the electron solvation and thermalization is over). These normalized kinetics begin to diverge only after the first 40−50 ps. At 500 ps, this divergence is very large: the probability $\Omega(t)$ of the electron survival rapidly decreases at higher ionic strength. The same behavior is observed in all cases: for sodium perchlorate and sodium sulfate solutions of bromide and for sodium perchlorate solutions of iodide. In the latter case, data at higher ionic strength show the same trend but with poorer signal-to-noise ratio, and thus have been omitted from Figure 5.

To a first approximation, the $t > 5$ ps kinetics shown in Figures 4 and 5 are biexponential, [2−7] and the escape probability Ω_∞ for $t \rightarrow \infty$ can be readily estimated from the corresponding least-squares fits (as explained in section 3.4.3, a more complex type of fit has actually been used, but the main result does not depend on the specific prescribed profile of the kinetics). These escape probabilities are plotted vs the ionic strength of the corresponding salt solutions in Figure 6a. The survival probability of the geminate pair decreases linearly with the ionic strength with a slope (expressed in relative terms) of ca. 9% per 1 M for bromide (200 nm photoexcitation) and ca. 12% for iodide (228 nm photoexcitation). This slope is close to the slope

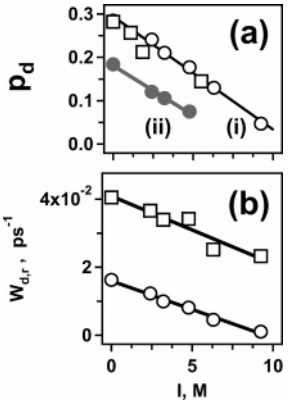

Figure 6. Simulation parameters used to fit the data shown in Figures 4b and 12S (for bromide) and Figure 5b (for iodide) vs the nominal ionic strength I of the aqueous solution. (a) The escape probability p_d of the photoelectron in (i) 200 nm photoexcitation of bromide in sodium sulfate (open squares) and sodium perchlorate (open circles) solutions and (ii) 228 nm photoexcitation of iodide in sodium perchlorate (filled circles). (b) Dissociation (W_d, circles) and recombination (W_r, squares) rate constants for caged (Br, e_{aq}^-) pairs plotted vs ionic strength of concentrated sodium perchlorate solutions.

of 8−11% per 1 M observed for the decrease in QY of free electron in 248 nm photoexcitation of iodide and sulfite (Figure 3(c)). Thus, the answer to the question formulated at the end of section 3.3 is that the QY of free electron decreases as a function of the ionic strength due to the decrease in the fraction of electrons that escape geminate recombination; the prompt yield of thermalized electrons does not change significantly with the addition of salts.

Interestingly, the transformations of the kinetics with the increasing ionic strength shown in Figures 4 and 5 are exactly opposite to the transformations observed for the decay kinetics in 200 nm photoexcitation of hydroxide with increasing temperature.[7] An increase in the temperature red-shifts the spectra of halide/pseudohalide anions and the hydrated electron and increases Ω_∞; the main difference between the effect of the salt addition and the effect of the temperature increase is that for the latter the normalized kinetics diverge on the time scale of tens rather than hundreds of picoseconds. [7] Still, the overall behavior is strikingly similar: the effect of increasing the ionic strength largely resembles the effect of lowering the solution temperature.

We will return to the interpretation of the geminate recombination kinetics in section 3.4.3. For now, it suffices to note that the ionic strength effect on the geminate recombination is slow to develop: for electrons photodetached from halide anions it takes 300−500 ps for this effect to develop fully. As shown in the next section, for other photosystems this time lag is even longer.

3.4.2. Sulfite and Hydroxide. Figure 7a shows the decay kinetics of electrons obtained in 200 nm photoexcitation of 40 mM sulfite in concentrated Na_2SO_4 solution (nonnormalized kinetics are shown in Figure 14S(a)). The thermalization kinetics follow the same transformations as those observed for bromide in $NaClO_4$ solutions (albeit on a smaller scale, due to a smaller blue shift of the hydrated electron band in the sodium sulfate solution, Figure 5S). Normalization of the transient absorbance from the hydrated electron at $t = 5$ ps by the molar absorptivity of the electron at 800 nm (which linearly decreases with the increase in ionic strength, see Figures 13S(a) and 13S(c)) shows that the prompt yield of the thermalized electrons change very little in these sodium sulfate solutions (as was also observed for bromide, see section 3.4.1). When these kinetics are

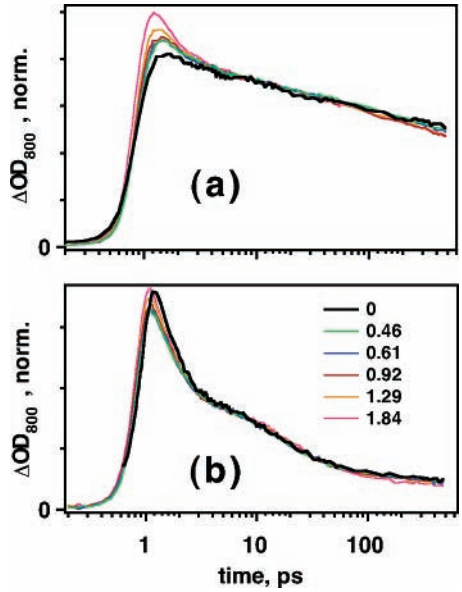

Figure 7. Normalized 200 nm pump−800 nm probe kinetics of photoelectron generated by photolysis of (a) 40 mM Na_2SO_3 and (b) 200 mM KOH in concentrated sodium sulfate solutions. The molarity of sulfate is given in the color scale. These kinetics were normalized at $t = 5$ ps. See Figure 14S for nonnormalized kinetics.

normalized at 5−10 ps (at the end of the thermalization kinetics) the "tails" of these kinetics ($t > 100$ ps) barely diverge, though one can see that at $t = 500$ ps the escape of electrons in water is more efficient than this escape in 1.83 M Na_2SO_4 solution. Similar behavior was observed for 200 nm photoexcitation of the sulfate anion in concentrated Na_2SO_4 solutions (see section 3S and Figures 9S(a) and 10S therein): the escape probability of the electron at $t = 500$ ps for 1.8 M solution was ca. 12% lower than for 0.74 M solution.

For hydroxide, the changes in the escape probability are even smaller than for sulfite. As shown in Figure 14S(b), the changes in the kinetics are confined to thermalization dynamics; the normalized kinetics after 10 ps are nearly the same, with barely perceptible divergence after the first 200 ps (Figure 7b). The lack of an ionic strength effect on these $t < 500$ ps kinetics is not completely unexpected: Crowell and co-workers [7,8] have studied the effect of addition 1−10 M KOH on the electron and OH radical dynamics in 200 nm photoexcitation of hydroxide. No effect was observed. Thus, for hydroxide and sulfite, not only there is no effect of the ionic strength on the prompt yield but there appears to be little decrease in the survival probability of the geminate pair in the first 500 ps after the electron detachment.

In section 3.3, a large effect of the ionic strength on the *free electron* yield was observed for 193 nm photoexcitation of hydroxide and 248 nm photoexcitation of sulfite. Since our ultrafast measurements suggest that the initial quantum yield of hydrated electron does not change with ionic strength of the solution, it follows that the kinetics obtained at different concentrations of the salt should eventually diverge. For sulfite and sulfate, only the initial stages of this divergence were observed in the first 500 ps. Apparently, what distinguishes hydroxide, sulfate, and sulfite from halide anions is that the time scale on which the geminate dynamics diverge (eventually approaching similar Ω_∞) is much *longer:* the full effect is perhaps attained on the time scale of a few nanoseconds.

3.4.3. Kinetic Simulations for Halide Anions. As stated in the Introduction, electron dynamics observed in the previous studies of electron photodetachment from monovalent aqueous

anions broadly conformed to the MFP model. One particular realization of this model is the semianalytical theory of Shushin.[9] We refer the reader to refs 7 and 9 for a rigorous formulation of that model. Very briefly, Shushin[9] showed that, under most realistic conditions, the time dependent survival probability $\Omega(t)$ of a geminate pair is not sensitive to the radial profile $U(r)$ of the MFP per se. Rather, this probability depends on a few global parameters that can be analytically derived from this potential. These parameters are the Onsager radius a (at which the potential equals the Boltzmann energy, $U(a) \approx -kT$) and the first-order rates W_r and W_d for the recombination and dissociation from the potential well ($r < a$), respectively (so that $W = W_d + W_r$ is the total rate of the decay of pairs inside the potential well). From these three parameters and the mutual diffusion coefficient D of the pair, two dimensionless parameters can be obtained: the survival probability $p_d = W_d/W$ of the geminate pair generated inside the potential well ($\Omega_\infty = p_d$) and $\alpha = p_d(Wa^2/D)^{1/2}$, which characterizes how rapidly the short-term exponential kinetics $\Omega(t) \propto \exp(-Wt)$ transforms into long-term kinetics tailing as $p_d[1 + a/(\pi Dt)^{1/2}]$. The overall kinetics is given by a rather complex formula;[7,9] the important point is that all experimental traces observed so far can be fit by this formula, or its minor modification[7] that provides for the possibility that some geminate pairs are initially generated beyond the Onsager radius of the MFP.

The traces for Br^- shown in Figures 4b and 12S can also be simulated using Shushin's theory equations. Since for bromide no difference was observed between the kinetics obtained using 200 and 228 nm photoexcitation,[6] we assumed that addition of salts does not change the initial distribution of electrons around bromine atom and assumed that this initial distribution is entirely confined within the potential well.

Figure 12S shows a global fit of normalized kinetics for the Br^-/Na_2SO_4 photosystem using Shushin's theory equations. In these least-squares fits, parameters W^{-1} and α were assumed to be constant (19.5 ps and 0.552, respectively); only the survival probability $\Omega_\infty = p_d$ was allowed to change (Figure 6a gives the optimum values for this parameter as a function of the ionic strength). Although this way of fitting the kinetic data obviously works, all it really conveys is that the change in p_d is the main cause for the kinetic transformations shown in Figures 4b and 12S. Indeed, since α and p_d explicitly depend on W, it is difficult to explain how the constancy of W and α can be reconciled with a large change in p_d, even if the fit quality is good.

For sodium perchlorate solutions, the range of the kinetic change is greater, and it becomes apparent that this constancy with the ionic strength is not maintained: it is impossible to find optimum parameters W and α for which a change in p_d alone accounts for the observed kinetic transformations. Assuming constancy of the Onsager time $\tau_c = a^2/D$ with the ionic strength, rate constants W_d and W_r can be determined from the least-squares fits for individual kinetic traces in Figure 4b. As shown in Figure 6b, these optimum rate constants, the decay constant W, and the survival probability p_d for bromide, all decrease linearly with the ionic strength. The same behavior was observed for iodide (Figures 5b and 6a) for which the optimum W^{-1} increases from 14.3 ps in the aqueous solution to 16.7 ps in 4.8 M $NaClO_4$ solution.

Since W_r and W_d are complex functions of the potential $U(r)$,[7,9] it is impossible (in the framework of Shushin's theory) to pinpoint what specific modifications of the MFP are required to obtain the changes shown in Figure 6b. Provided that the Onsager radius of the MFP does not change with ionic strength, only lowering of the reduced potential energy $U(r)/kT$ (i.e., making the MFP more attractive) can decrease both of these two rate constants. Thus, the most general conclusion that can be made from fitting these kinetics using the MFP model in its formulation by Shushin is that addition of salts strengthens the attraction between the electron and halogen atom. This partially accounts for the qualitative similarity of the temperature effect and the ionic strength effect: increase in the temperature *decreases* this reduced potential energy $U(r)/kT$ and increases W_d.

4. Discussion

The following picture emerges from the results of section 3: Addition of molar concentration of salts to aqueous solutions of CTTS anions does not change the prompt quantum yield for the formation of hydrated electron, but rather, it decreases the survival probability of the geminate electron. Monovalent and polyvalent anions exhibit exactly the same behavior in free electron yields; the anticipated qualitative difference in the effect of ion screening on the two types of geminate pairs originating from these anions (section 1) was not observed. For the same ionic strength, the decrease in the limiting survival probability Ω_∞ of hydrated electron is similar for all anions (Figures 3c and 6a), but the rate by which the full ionic strength effect is attained appears to vary considerably among the photosystems. For two photosystems only (bromide anion photoexcited by 200 nm light and iodide anion photoexcited by 228 nm light), we were able to observe the limiting value of the survival probability in 500−700 ps (which was our observation window, Figures 4 and 5). For these two halide anions, the kinetics obtained at different ionic strengths started to diverge after 50 ps, when the fast exponential component was over, and the effect developed fully on the time scale of hundreds of picoseconds, when the decay of the electron was controlled by diffusional migration of the geminate partners to the bulk and their re-encounters. It is safe to conclude that the ionic strength effect develops slowly and requires many such re-encounters. Analysis of the kinetics for halide photosystems in the framework of the MFP well model of Shushin[9] given in section 3.4.3 suggests that the changes in the kinetics can be rationalized in terms of the increased attraction between the geminate partners in high ionic strength solutions.

Some of these observations broadly agree with the anticipated effect of charge screening. For polyvalent anions, a decrease in the long-range repulsion between the geminate partners facilitates their recombination thereby decreasing the survival probability of the electron.[10] Because this repulsion is already screened by water, the effect can be observed only at high concentration of the screening ions and only when the partners are close; thus, many reencounters are needed. Since photoexcited polyvalent anions (unlike monovalent anions) yield a broad distribution of separation distances between the electron and its geminate partner[8,10,49] the average distance between these partners is always very long (2−3 nm) and the screening (which is a relatively short-range effect) takes a longer time to perturb the geminate dynamics.

The main observation here is more difficult to rationalize. For monovalent anions, the MFP potential is attractive and thought to originate through weak electrostatic interactions between the geminate partners.[11−13] Screening of these interactions would make the attractive force weaker thereby reducing the efficiency of recombination and increasing the survival probability. This, apparently, does not happen. The most difficult observation to accommodate is that photosystems having different overall MFPs all show a similar relative decrease in

the survival probability when this potential is modified by intervening ions. In principle, the decrease in the survival probability for pairs originating from monovalent anions can be "explained" within the MFP model with ion screening. For example, it can be postulated that the reactivity of close pairs systematically increases with the ion concentration (e.g., due to pairing of the electron with a cation) and this effect counteracts the weakening of the attractive potential between the partners (though this rationale is incompatible with the $W_{r,d}$ data of Figure 6b). According to our viewpoint, such modifications are both forced and misguided because the similarity of the ionic strength effect for various photosystems emerges only as a consequence of fine-tuning of the model parameters in each particular case. Can something other than the ion screening cause the ionic strength effect? Below, we consider three alternate scenarios in detail.

The first scenario is that the ionic strength effect originates through narrowing of the initial distribution of the electrons. The idea is that an addition of salt causes a blue shift in the absorption spectrum of an anion and therefore is equivalent to photoexcitation of this anion (in water) at a lower energy. Since it is known that for some anions an increase in the excitation energy causes more electrons to escape (due to the broadening of the electron distribution via enhanced direct ionization),[6,14,18] the salt-induced blue shift causes the opposite effect. Though this scenario cannot be excluded for sulfite[6] and hydroxide,[6,7] it can be completely excluded for iodide and bromide because for these two halide anions no wavelength dependence was observed to the red of their CTTS band maxima.[2,6,14]

The second scenario is that the ionic strength effect originates via a purely kinematic effect, such as an increase in the solution viscosity and/or the ionic atmosphere drag on the electron diffusion. The drag of a slowly migrating ionic atmosphere on the rapidly migrating ion is a well-known effect: the ionic atmosphere needs to readjust itself as the fast ion (e.g., hydrated electron) migrates. In the Debye−Hückel theory of aqueous electrolytes (applicable to $I < 0.1$ M), the relaxation time for the ionic atmosphere is $55/I$ ps; that is, at the upper limit of validity of this theory, it takes the ionic atmosphere ca. 500 ps to relax. [7] Perhaps, this relaxation time continues to decrease in concentrated solutions (although this trend is opposed by slowing of the ion diffusion (Figure 1S(b)) and ion pairing (Figure 2S(b)). Thus, it is possible that the diffusion coefficient of the electron systematically decreases with delay time t in the observation window of our ultrafast kinetic experiments. However, one would expect that the drag on the electron diffusion develops on the same time scale in all photosystems. Almost complete lack of kinetic variation with the ionic strength for some photosystems (e.g., for hydroxide and sulfite, see refs 7 and 8 and section 3.4.2) suggests that this effect is relatively minor, at least on a subnanosecond time scale. Furthermore, although a time-dependent (or decreased) electron diffusivity would change the temporal profile of the kinetics, it cannot change the survival probability: in the MFP model, the latter depends on the potential only. Thus, this scenario should also be rejected.

The third and last scenario is ion association. Before proceeding any further, let us consider the existing explanations for salt-induced blue shift in the absorption spectra of halide (e.g., iodide) anions and the hydrated electron. Both of these species exhibit very similar blue shifts for a given salt concentration (cf. Figures 2b and 6S(b)). Since the original suggestion by Stein and Treinin,[33] most authors accounted for this effect by constriction of the solvation cavity around the anion/electron (some more exotic explanations have been considered by Blandamer and Fox),[1] though the cause for this constriction has never been specified. The blue shift of the solvated/trapped electron spectrum is observed both in liquid and solid vitreous salt solutions, such as alkaline glasses.[50] For the latter, electron spin−echo envelope modulation (ESEEM) spectroscopy provides direct evidence for the inclusion of sodium cation in the first solvation shell of the trapped electron through the observation of dipole and Fermi coupling of the unpaired electron to the spin of ^{23}Na nucleus.[51] In alkaline earth salt aqueous glasses[50] and THF solutions,[52] electrons associated with one or several cations can be distinguished by optical spectroscopy. In most of these glasses, the visible band coexists with an IR band that gradually shifts to the blue; for alkaline glasses the visible band itself shifts to the blue on a sub-millisecond time scale.[50] Many authors speculated that the cations are actively involved in the trapping site of the electron causing the delayed trap deepening, and specific "ionic lattice trap" models detailing this involvement were formulated by Hilczer et al.[53] and Bartzak et al.[54] In short, there is much evidence pointing to structural involvement of alkali cations in electron dynamics observed for low-temperature glassy solutions.

We suggest that the same process occurs in liquid aqueous solutions at room temperature: sodium cations are included in the solvation shell of the electron. The thermalization kinetics given in section 3.4.1 indicate that in concentrated salt solutions, the electron spectra blue shift on a time scale similar to that of electron thermalization in pure water. This means that the postulated association of sodium cation(s) with the electron occurs very rapidly, in less than 5 ps. Assuming a diffusion controlled association of the free sodium cation and the electron and taking the diffusion coefficients for the electron (in water) and the sodium cation as 4.9×10^{-5} and 1.2×10^{-5} cm^2/s, respectively, the association in 1 M $NaClO_4$ would take ca. 45 ps (assuming no clustering of the sodium cations around the parent anion), whereas the blue shift in the electron spectrum develops in <5 ps. This estimate suggests that the cation associated with the electron originates either from the dense part of the ion atmosphere around the parent anion or from a cation that is associated with this anion (thereby causing the blue shift of the anion spectrum). That the latter association occurs to some degree (at least, for polyvalent anions) via the formation of solvent-separated ion pairs, follows from many independent observations (e.g., see section 3.1) which point to such pairs as the main entity in concentrated solutions. The association of e_{aq}^- and Na^+ has been previously suggested by Gauduel and co-workers to account for electron thermalization and subpicosecond dynamics of geminate pairs generated in 2-photon excitation of aqueous chloride. [55]

Thus, we suggest that in concentrated salt solutions both the anion and the electron are associated with alkali cations and that the cation associated with the parent anion (or included in the inner part of the ionic atmosphere around this parent anion) is passed to the electron in the course of CTTS state dissociation on subpicosecond time scale, possibly, in the manner envisioned by Gauduel and co-workers.[55] The fraction of associated anions and electrons rapidly increases with the ion concentration. This association makes the short-range potential more attractive, for all anions, including polyvalent anions. A possible cause for this effect is the increased attraction between the radical/atom and hydrated electron bridged by a cation; rather than screening the weak attractive forces, such a cation might bind these species together by excluding the screening water dipoles.

Although this picture is incomplete, it contains a verifiable rationale: the ionic strength effect originates from the modulation of short-range attraction between the geminate partners rather than long-range ion screening. A modification of short-range MFP for the ($X^{(n-1)-}$•, e_{aq}^-) pair due to the involvement of alkali cation(s) in the solvation of the parent anion (X^{n-}) and the electron e_{aq}^- is postulated. For reasons not entirely understood, this association makes the attractive MFP interaction stronger thereby causing all of the changes observed in section 3.4. Only detailed molecular dynamics simulation of this charge separation process (along the lines of refs 12, 19, 56, 57, and 58) can shed more light on the mechanism. The first step in this direction has already been taken by Spezia et al.,[59] who used the umbrella sampling approach of Borgis and Staib[12,13] to obtain the MFP for interaction of hydrated electron and Na^+. These simulations suggests the existence of a contact (Na^+, e_{aq}^-) pair with the average distance of ca. 0.2 nm and the binding energy of 3−4 *kT*.

5. Conclusion

It is shown that in concentrated solutions of $NaClO_4$ and Na_2SO_4 the quantum yield for (free) electron photodetachment from CTTS anions (such as I^-, OH^-, ClO_4^-, and SO_3^{2-}) decreases linearly by 6−12% per 1 M ionic strength. In 9 M sodium perchlorate solution, this QY decreases by roughly 1 order of magnitude. Ultrafast kinetic studies on 200 nm photon-induced electron detachment from Br^-, I^-, HO^-, and SO_3^{2-} suggest that the prompt yield of thermalized electron in these solutions does not change; the ionic strength effect wholly originates in the decrease in the survival probability of geminate pairs. Kinetically, this effect manifests itself in much the same way as the temperature effect studied previously;[7] that is, addition of salt and decrease in temperature cause similar changes in the electron dynamics. In this respect, the ionic strength effect on the QY follows the same pattern as the shift in the absorption spectra of the CTTS anions and the hydrated electron itself.[1,34,36]

Within the framework of the recently proposed MFP model of charge separation dynamics in CTTS photosystems,[2,7] the observed changes can be explained by an increase in the short-range attractive potential between the geminate partners (possibly, due to the association of sodium cation(s) with the electron and the parent anion); ion screening plays minor role. The precise mechanism for modification of the MFP by these cations is presently unclear, although electron thermalization kinetics for halide photosystems suggest that the sodium cation associated with the parent anion is passed to the photodetached electron.[55] Further advance in the understanding of the ionic strength effect is predicated on the development of a molecular dynamics model that directly includes the interactions of the geminate partners with cations in the ionic atmosphere.

Acknowledgment. We thank Prof. B. J. Schwartz of UCLA and Dr. S. V. Lymar of BNL for many useful discussions. The research at the ANL was supported by the Office of Science, Division of Chemical Sciences, US-DOE under Contract Number W-31-109-ENG-38. The research at USC was supported by the David and Lucile Packard Foundation. S.E.B. is a Cotrell Scholar of the Research Corporation.

Supporting Information Available: A PDF file containing the following Supporting Information: (1). The effect of salts on the absorption of hydrated electron (pulse radiolysis study). (2). Quantum yields for electron and I_2^- formation in 248 nm photolysis of iodide. (3). Transient picosecond kinetics of photoelectron observed in 200 nm photolysis of sodium perchlorate and sodium sulfate solutions. (4) Figures 1S−14S with captions. This material is available free of charge via the Internet at http://pubs.acs.org.

References and Notes

(1) Sauer, M. C., Jr.; Crowell, R. A.; Shkrob, I. A. *J. Phys. Chem. A* **2004**, *108*, 5490; Part 1 of this series.

(2) Kloepfer, J. A.; Vilchiz, V. H.; Lenchenkov, V. A.; Chen, X.; Bradforth, S. E. *J. Chem. Phys.* **2002**, *117*, 776.

(3) Vilchiz, V. H.; Kloepfer, J. A.; Germaine, A. C.; Lenchenkov, V. A.; Bradforth, S. E. *J. Phys. Chem. A* **2001**, *105*, 1711.

(4) Kloepfer, J. A.; Vilchiz, V. H.; Germaine, A. C.; Lenchenkov, V. A.; Bradforth, S. E. *J. Chem. Phys.* **2000**, *113*, 6288.

(5) Kloepfer, J. A.; Vilchiz, V. H.; Lenchenkov, V. A.; Bradforth, S. E. In *Ultrafast Phenomena XIII*; Miller, D., Ed.; Springer-Verlag, Berlin, 2003, pp 471. Kloepfer, J. A.; Vilchiz, V. H.; Lenchenkov, V. A.; Bradforth, S. E. In *Liquid Dynamics: Experiment, Simulation, and Theory*; American Chemical Society: Washington, DC, 2002; Vol. 820, pp 108. Kloepfer, J. A.; Vilchiz, V. H.; Lenchenkov, V. A.; Bradforth, S. E. *Chem. Phys. Lett.* **1998**, *298*, 120.

(6) Lian, R.; Oulianov, D. A.; Crowell, R. A.; Shkrob, I. A.; Chen, X.; Bradforth, S. E. in preparation, to be submitted to *J. Phys. Chem. A* (Part 3 of the series).

(7) Lian, R.; Crowell, R. A.; Shkrob, I. A.; Bartels, D. M.; Chen, X.; Bradforth, S. E. *J. Chem. Phys*. **2004**, *120*, 11712.

(8) Lian, R.; Crowell, R. A.; Shkrob, I. A.; Bartels, D. M.; Oulianov, D. A.; Gosztola, D. *Chem. Phys. Lett.* **2004**, *389*, 379.

(9) Shushin, A. I. *J. Chem. Phys*, **1992**, *97*, 1954; *Chem. Phys. Lett.* **1985**, *118*, 197; *J. Chem. Phys.* **1991**, *95*, 3657.

(10) Lenchenkov, V. A.; Chen, X.; Vilchiz, V. H.; Bradforth, S. E. *Chem. Phys. Lett.* **2001**, *342*, 277.

(11) Vilchiz, V. H. *Electron Photodetachment from Singly Charged Anions*; Ph. D. dissertation, University of Southern California, 2002. Vilchiz, V. H.; Kloepfer, J. A.; Lenchenkov, V. A.; Bradforth, S. E., manuscript in preparation.

(12) Borgis, D.; Staib, A. *J. Chem. Phys.* **1996**, *104*, 4776 and 9027.

(13) Gaigeot, M. P.; Borgis, D.; Staib, A. *J. Mol. Liq.* **2000**, *84*, 245.

(14) Chen, X.; Kloepfer, J. A.; Bradforth, S. E.; Lian, R.; Crowell, R. A.; Shkrob, I. A. (in preparation).

(15) Vilchiz, V. H.; Chen, X.; Kloepfer, J. A.; Bradforth, S. E. *Radiat. Phys. Chem.* **2004** in press.

(16) Barthel, E. R.; Martini, I. B.; Schwartz, B. J. *J. Chem. Phys.* **2000**, *112*, 9433. Barthel, E. R.; Martini, I. B.; Keszei, E.; Schwartz, B. J. *J. Chem. Phys.* **2003**, *118*, 5916. Barthel, E. R.; Martini, I. B.; Keszei, E.; Schwartz, B. J. *J. Chem. Phys.* **2001**, *105*, 12230.

(17) Martini, I. B.; Barthel, E. R.; Schwartz, B. J. *J. Am. Chem. Soc.* **2002**, *124*, 7622; *Science* **2001**, *293*, 462. Martini, I. B.; Schwartz, B. J. *Chem. Phys. Lett.* **2002**, *360*, 22.

(18) Barthel, E. R.; Schwartz, B. J. *Chem. Phys. Lett.* **2003**, *375*, 435.

(19) Smallwood, C. J.; Bosma, W. B.; Larsen, R. E.; Schwartz, B. J. *J. Chem. Phys.* **2003**, *119*, 11263.

(20) Lenchenkov, V. A. *Femtosecond Dynamics of Electron Photodetachment from coordinated anions: hexaferrocyanate and tribromocuprate in solution*; Ph. D. dissertation, University of Southern California, 2002.

(21) Elliot, A. J.; Ouellette, D. C.; Stuart, C. R. *The Temperature Dependence of the Rate Constants and Yields for the Simulation of the Radiolysis of Heavy Water*, AECL report 11658; AECL Research, Chalk River Laboratories: Chalk River, Ontario, Canada, 1996.

(22) Jou, F.-Y.; Freeman, G. R. *Can. J. Chem.* **1979**, *57*, 591.

(23) Shkrob, I. A.; Sauer, M. C., Jr. *J. Phys. Chem. A* **2002**, *106*, 9120.

(24) Zaytsev, I. D.; Aseyev, G. G. *Properties of Aqueous Electrolytes*; CRC Press: Boca Raton, FL, 2000; pp 7, 164, and 924.

(25) *Solubilities of Inorganic and Organic Compounds. v. 1. Binary Systems. Part I*; Stephen, H.; Stephen, T., Eds.; Pergamon: New York, 1963.

(26) Kohner, H. *Z. Phys. Chem. B* **1928**, *1*, 427.

(27) *Handbook of Chemistry and Physics*, 69th ed.; Weast, R. C., Astle, M. J., Beyer, W. H., Eds.; CRC Press: Boca Raton, FL, 1988.

(28) Daly, F. P.; Brown, C. W.; Kester, D. R. *J. Phys. Chem.* **1972**, *76*, 3664.

(29) Buchner, R.; Capewell, S. G.; Hefter, G.; May, P. M. *J. Phys. Chem. B* **1999**, *103*, 1185.

(30) Fischer, F. H. *J. Solution. Chem.* **1975**, *4*, 237. Gilligan, T. J., III.; Atkinson, G. *J. Phys. Chem.* **1980**, *84*, 208.

(31) Weingärtner, H.; Price, W. E.; Edge, A. V. J.; Mills, R. *J. Phys. Chem.* **1993**, *97*, 6290.

(32) Blandamer, M. J.; Fox, M. F. *Chem. Rev.* **1970**, *70*, 59.

(33) Stein, G.; Treinin, A. *Trans. Faraday Soc.* **1960**, *56*, 1393.

(34) Fox, M. F.; Hayon, E. *J. Chem. Soc., Faraday Trans. 1* **1976**, *72*, 1990.

(35) Anbar, M.; Hart, E. J. *J. Phys. Chem.* **1965**, *69*, 1244. see also Asaad, A. N.; Chandrasekhar, N.; Nashed, A. W.; Krebs, P. *J. Phys. Chem. A* **1999**, *102*, 6339 and references therein.

(36) Hart, E. J.; Anbar, M. *The Hydrated Electron*; Wiley-Interscience: New York, 1970.

(37) Dainton, F. S.; Fowles, P. *Proc. R. Soc. A* **1965**, *287*, 312 and 295.

(38) Iwata, A.; Nakashima, N.; Kusaba, M.; Izawa, Y.; Yamanaka, C. *Chem. Phys. Lett.* **1993**, *207*, 137.

(39) Elliot, A. J.; Sopchyshyn, F. C. *Int. J. Chem. Kinet.* **1984**, *16*, *1247*. Devonshire, R.; Weiss, J. J. *J. Phys. Chem.* **1968**, *72*, 3815. Zehavi, D.; Rabani, J. *J. Phys. Chem.* **1972**, *76*, 312.

(40) See, for example: Tasker, P. W.; Balint-Kurti, G. G.; Dixon, R. N. *Mol. Phys.* **1976**, *32*, 1651.

(41) Jortner, J.; Ottolenghi, M.; Stein, G. *J. Phys. Chem.* **1964**, *68*, 247.

(42) Ohno, S. *Bull. Chem. Soc. Jpn.* **1967**, *40*, 1776 and 1770.

(43) Cohen; S. R.; Plane, R. A. *J. Phys. Chem.* **1957**, *61*, 1096. Davies, C. W. *J. Am. Chem. Soc.* **1937**, *59*, 1760.

(44) By using sufficiently concentrated bromide solutions (in section 3.4.2, sulfite solutions) for which the optical density at 200 nm across the jet is much greater than unity, it is possible to completely eliminate the variation of the initial electron concentration with the molar absorptivity of the anion: since all 200 nm photons are absorbed by the anion (regardless of the sodium perchlorate and sulfate concentrations), the prompt electron concentration depends on the quantum efficiency of electron detachment only. The concentration of the anions of interest in these concentrated saline solutions should also be sufficiently high so that the photoionization of sulfate and perchlorate by 200 nm photons is fully suppressed (see section 3S).

(45) Lian, R.; Crowell, R. A.; Shkrob, I. A., submitted to *J. Phys. Chem. A*; abstract available in Abstracts of Papers, 226th ACS National Meeting, New York, United States, September 7−11, 2003; American Chemical Society: Washington, DC, 2003; preprint available on http://www.arXiv.org/abs/physics/0405047.

(46) See, for example: Hertwig, A.; Hippler, H.; Unterreiner, A.-N. *J. Phys. Condens. Matter* **2000**, *12*, A165. Pépin, C.; Goulet, T.; Houde, D.; Jay-gerin, J.-P. *J. Phys. Chem. A* **1997**, *101*, 4351. Laenen, R.; Roth, T.; Laubereau, A. *Phys. Rev. Lett.* **2000**, *85*, 50. Assel, M.; Laenen, R.; Laubereau, A. *J. Phys. Chem. A* **1998**, *102*, 2256. Shi, X.; Long, F. H.; Lu, H.; Eisenthal, K. B. *J. Phys. Chem.* **1996**, *100*, 11903.

(47) Hertwig, A.; Hippler, H.; Unterreiner, A.-N. *Phys. Chem. Chem. Phys.* **2002**, *4*, 4412.

(48) Crowell, R. A.; Lian, R.; Shkrob, I. A.; Qian, J.; Oulianov, D. A.; Pommeret, S. *J. Phys. Chem. A* **2004**, *108*, 9105.

(49) Kee, T. W.; Son, D. H.; Kambhampati, P.; Barbara, P. F. *J. Phys. Chem. A* **2001**, *105*, 8434.

(50) Kroh, J. In *Pulse Radiolysis*; Tabata, Y., Ed.; CRC Press: Boca Raton, FL, 1990; Chapter 16, pp 358.

(51) Dikanov, S. A.; Tsvetkov, Y. D. *Electron Spin−Echo Envelope Modulation (ESEEM) Spectroscopy*; CRC Press: Boca Raton, FL, 1992.

(52) Renou, F.; Archirel, P.; Pernot, P.; Levy, B.; Mostafavi, M. *J. Phys. Chem. A* **2004**, *108*, 987.

(53) Hilcer, M.; Bartczak, W. M.; Sopek, M. *Radiat. Phys. Chem.* **1985**, *26*, 693.

(54) Bartzak, W. M.; Hilczer, M.; Kroh, J. *Radiat. Phys. Chem.* **1981**, *17*, 431 and 481.

(55) For the ultrafast dynamics of the tentative ($Cl^{\bullet}$,e_{aq}^{-} ...Na^{+}) complexes and the discussion of possible mechanisms for rapid in-cage charge separation in concentrated H^{+}, Li^{+}, and Na^{+} chloride solutions, see: Gauduel, Y.; Gelabert, H. *Chem. Phys.* **2000**, *256*, 333. Gelabert, H.; Gauduel, Y. *J. Phys. Chem.* **1996**, *100*, 13993. Gauduel, Y.; Gelabert, H.; Ashokkumar, M. *Chem. Phys.* **1995**, *197*, 167. Similar mechanisms were also suggested by these workers for divalent cations, such as Mg^{2+} and Cd^{2+}, see: Gauduel, Y.; Hallou, A.; Charles, B. *J. Phys. Chem.* **2003**, *107*, 2011. Gauduel, Y.; Hallou, A. *Res. Chem. Intermed.* **2001**, *27*, 359. Gauduel, Y.; Sander, M.; Gelabert, H. *J. Phys. Chem. A* **1998**, *102*, 7795.

(56) Sheu, W.-S.; Rossky, P. J. *Chem. Phys. Lett.* **1993**, *202*, 186 and 233; *J. Am. Chem. Soc.* **1993**, *115*, 7729; *J. Phys. Chem.* **1996**, *100*, 1295.

(57) Borgis, D.; Staib, *A. Chem. Phys. Lett.* **1994**, *230*, 405; *J. Chim. Phys.* **1996**, *93*, 1628; *J. Phys.: Condens. Matter* **1996**, *8*, 9389; *J. Mol. Struct.* **1997**, *436*, 537; *J. Chem. Phys.* **1995**, *103*, 2642

(58) Bradforth, S. E.; Jungwirth, P. *J. Phys. Chem. A* **2002**, *106*, 1286.

(59) Spezia, R.; Nicolas, C.; Archirel, P.; Boutine, A. *J. Chem. Phys.* **2004**, *120*, 5262.